Rakhimberdiev Ravshanbek, Magistr
Tashkent State Technical University
named after Islam Karimov

Husanov Bakhtiyor, teacher
Tashkent State Technical University
named after Islam Karimov

Usmanov Eldar, teacher
Tashkent State Technical University
named after Islam Karimov

INVESTIGATION OF A PLC-BASED CONTACTLESS VOLTAGE RELAY

Abstract. A contactless voltage relay for a single-phase 220 V, 50 Hz low-voltage network is studied. The device is built around a galvanically isolated true-RMS transducer, a programmable logic controller (PLC) and a zero-cross solid-state relay (SSR). The functional structure and the control algorithm combine analog-input scaling, digital IIR filtering, separate trip and restoration thresholds, two different time delays and fail-safe diagnostics of the measuring channel. Discrete-time simulation with a 10 ms step is used to estimate the measurement error, the operating time and the immunity of the output to threshold-adjacent oscillations. During a 10 s oscillation of 198 ± 3 V the non-hysteretic algorithm changes state 159 times, whereas the proposed algorithm does not change state at all, while retaining a trip time of 0.13 s. The digital filter reduces the standard deviation of the measured voltage by a factor of about 2.6 without introducing a systematic bias. The limitations of the computational model and a programme of experimental validation are discussed.

Keywords: PLC, contactless voltage relay, undervoltage, overvoltage, solid-state relay, zero-cross switching, hysteresis, IIR filter, TON timer, electrical equipment protection.

Introduction

Voltage deviations in low-voltage networks can increase motor current, reduce electromagnetic-device performance and cause unplanned equipment shutdowns. Reliable undervoltage and overvoltage protection therefore requires accurate measurement, decision making, time delay and switching in accordance with IEC 60255-1, IEC 60255-27 and IEC 60255-26 [1–3].

Conventional voltage relays use mechanical contacts that may switch repeatedly under near-threshold noise, causing wear and arcing. This study considers a contactless solution based on a PLC, an isolated RMS transducer and a zero-cross solid-state relay (SSR). The PLC provides adjustable settings, HMI monitoring and event logging according to IEC 61131-3 [5], while its scan cycle, measurement error and SSR delay affect total operating time [6]. Building on PLC-based and digital-relay studies [8–10], the proposed model combines IIR filtering, hysteresis, separate trip and restoration delays, and fail-safe diagnostics. It is intended to protect local single-phase 220 V, 50 Hz loads and does not replace certified substation protection.

1. Functional structure of the device

The functional structure of the proposed device is shown in Figure 1. The mains voltage is converted by a galvanically isolated true-RMS transducer into a 0–10 V DC signal, which is fed to the PLC analog input. The controller performs scaling, digital filtering, hysteresis-based decision making, time-delay processing, and diagnostics. A 24 V DC transistor output drives the optical input of the solid-state relay (SSR); consequently, the PLC output is not connected directly to the 220 V load circuit. The HMI/SCADA channel displays the settings, measured values, operating states, fault codes, and time-stamped events.

Galvanic isolation between the input and output circuits of the true-RMS transducer separates the PLC and the operator interface from the mains potential. The 24 V DC power supply is selected with a power margin sufficient for the controller, the low-voltage side of the sensor, and the SSR input. The SSR is selected not only according to the rated load current, but also with regard to inrush current, ambient temperature, heat-sink performance, and the manufacturer's derating curve. For a resistive AC load, zero-cross switching reduces conducted and radiated disturbances during energisation [7]. Because the off-state leakage current, on-state voltage drop, and heat dissipation of an SSR differ from those of a mechanical relay, a fast-acting fuse, a suitable heat sink, and, where necessary, an RC snubber or varistor are provided.

2. Measuring channel and digital filtering

The 0–10 V output of the 0–300 V transducer is acquired by the PLC as a digital code in the range 0…27648. Assuming that zero and full-scale calibration have been completed, the voltage at the k-th sample is determined as

$$U_k = U_{FS} \cdot x_k / 27648,\ U_{FS} = 300\ \text{V} \quad (1)$$

where x_k is the digital value of the analog input and UFS is the upper measuring limit of the transducer. On a physical test bench, the multiplicative coefficient k^c and additive coefficient b^c obtained from a two-point calibration are introduced into expression (1):

$$U_k = k_c \cdot U_{FS} \cdot x_k / 27648 + b_c. \quad (2)$$

If the code leaves the configured valid range, the analog module reports a diagnostic fault, or supervision of the sensor supply fails, the AI_FAULT flag is set and the SSR output is switched off. A frozen-value fault may be declared only when a separate plausibility or watchdog criterion is available; an unchanged voltage value alone is not sufficient evidence of sensor failure.

ADC quantisation and transducer noise may make the decision unstable near a threshold. Therefore, a first-order exponential infinite-impulse-response (IIR) filter is applied:

$$\bar{U}_k = \alpha \cdot U_k + (1 - \alpha) \cdot \bar{U}_{k-1},\ 0 < \alpha \le 1. \quad (3)$$

With $\alpha = 0.25$ and a sampling period $T_s = 10$ ms, the equivalent time constant of the filter is approximately 35 ms. Decreasing α improves noise suppression but delays fault detection; increasing α has the opposite effect. Consequently, α, the TON timer setting, and the sensor update period must be selected as a single dynamic chain. IEC 61000-4-30 defines methods for the reproducible assessment of power-quality parameters, including supply-voltage magnitude, dips, and swells [4]. However, the local protection model considered here is not claimed to be a Class A or Class S power-quality instrument.

3. Hysteretic protection logic and fail-safe state

For $U_n = 220$ V, the model adopts the trip thresholds Utrip,L = 198 V and Utrip,H = 242 V and the restoration thresholds Ures,L = 203 V and Ures,H = 237 V. A 5 V hysteresis band is therefore formed at both limits. For tripping, the out-of-range condition must persist continuously for 0.10 s, whereas for restoration the voltage must remain continuously within the narrower safe window for 1.0 s:

$$\text{TRIP} = [(\bar{U}_k < 198) \lor (\bar{U}_k > 242)] \land (t_{bad} \ge 0.10\ \text{s}), \quad (4)$$

$$\text{RESET} = [203 \le \bar{U}_k \le 237] \land (t_{safe} \ge 1.00\ \text{s}). \quad (5)$$

The state diagram of the logic is shown in Figure 2. While the load is energised, only the TRIP condition is evaluated. When the load is de-energised, both the RESET window and the re-energisation permission ResetPermit are required. ResetPermit may be generated by an authorised operator command or by an approved automatic-restart policy. This approach prevents the load from being energised in one scan and tripped in the next when the voltage oscillates around 198 or 242 V. An analog-input fault, a PLC diagnostic fault, or an emergency Stop signal produces the priority command DO_SSR = 0 in any state. In a physical device, the state of the hardware output during CPU STOP must also be verified against the PLC hardware configuration and the applicable safety requirements.

The algorithm can be expressed by the following abridged fragment in the Structured Text language defined by IEC 61131-3. An industrial program additionally includes timer instances, first-scan initialisation, range checking of settings, HMI access rights, fault latching, output-feedback diagnostics, and time-stamped archive blocks.

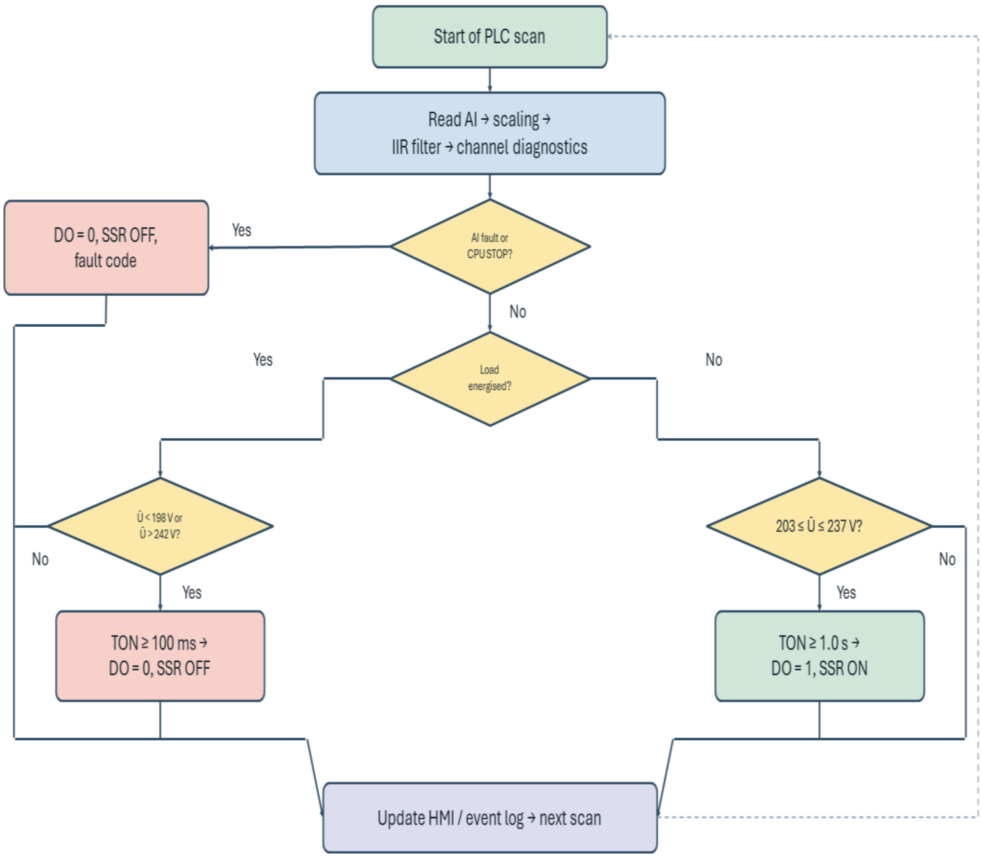

Figure 1 – Flowchart of the PLC algorithm with hysteresis, time delays, and priority fault handling

The total operating time of the device is the sum of the response times of the sensor, analog module, PLC scan, digital filter, programmed delay, and zero-cross switching stage:

$$t_{op} = t_{sens} + t_{AI} + t_{scan} + t_{filt} + t_{delay} + t_{zc}. \quad (6)$$

In a 50 Hz network, the component tzc lies within 0…10 ms when a zero-cross SSR is commanded to turn on. Turn-off occurs when the thyristor or triac current falls below the holding current; with an inductive load, the current zero may not coincide with the voltage zero. For this reason, the SSR selection in Table 1 applies to a resistive test load. Switching a motor or transformer requires a dedicated contactless contactor, an SSR designed for the relevant load type, or another appropriately rated switching device.

4. Advantages, limitations, and practical validation

The main advantage of the proposed solution is the ability to modify settings, archive events, perform remote monitoring, and store separate protection profiles for different loads on a single hardware platform. A contactless SSR eliminates mechanical power-contact wear under frequent switching, while the zero-cross function reduces electromagnetic disturbance when a resistive load is energised. Separate logging of the AI_FAULT, CPU_HEALTHY, ResetPermit, SSR command, and SSR feedback tags simplifies root-cause analysis after a trip.

Nevertheless, the computational model does not fully represent the following physical factors: the frequency response of the true-RMS transducer in the presence of mains harmonics; impulse overvoltages; SSR temperature derating and the possibility of a short-circuit failure mode; displacement of the current zero with an inductive load; operation during sag of the PLC and sensor supply; and the influence of the electromagnetic environment on installation cables. Because leakage current persists in the OFF state, an SSR cannot be regarded as an isolating device during maintenance; a mechanical isolator or circuit breaker must be retained for safe isolation.

To validate a physical prototype, the static error is first determined over the range 180…255 V using a calibrated AC source and a reference true-RMS voltmeter. The trip thresholds and operating-time dispersion are then measured for voltage dips and swells lasting 20, 40, 60, 100, 150, and 500 ms. A threshold-noise test, an assessment of the thermal regime during repeated switching, and checks under CPU STOP, analog-input circuit fault, and loss of the HMI communication link are also carried out. For a finished product, dielectric strength, temperature-rise performance, electromagnetic immunity, and product safety must be confirmed by an accredited laboratory in accordance with the applicable IEC 60255 requirements and IEC 61131-2, which applies to PLC equipment [1–3, 10].

Conclusion

A functional structure has been developed for a contactless voltage relay protecting a low-voltage load, based on a PLC, a galvanically isolated RMS transducer and a zero-cross SSR. The proposed solution combines scaling of the measuring channel, IIR filtering, separate hysteresis thresholds for tripping and restoration, two different TON time delays and fail-safe diagnostics. The main results of the computational experiment are as follows.

1. The operating time was 0.13 s for an undervoltage of 185 V and 0.13 s for an overvoltage of 255 V; a short dip of 60 ms did not cause nuisance tripping.

2. During an oscillation of 198 ± 3 V the non-hysteretic algorithm changed state 159 times in 10 s, whereas the algorithm with an IIR filter, a 5 V hysteresis band and a 100 ms TON timer did not change state at all.

3. Reconnection delayed by 1.01 s after the recovery of normal voltage limits repeated starting of the load during short-term recoveries.

4. Digital filtering reduced the standard deviation of the measured voltage by a factor of about 2.6, with a maximum relative error of the channel model of 0.17 %, which is considerably smaller than the adopted hysteresis width

References:

1. IEC 60255-1:2022. Measuring relays and protection equipment – Part 1: Common requirements. Geneva: International Electrotechnical Commission, 2022.

2. IEC 60255-27:2023. Measuring relays and protection equipment – Part 27: Product safety requirements. Geneva: IEC, 2023.

3. IEC 60255-26:2023. Measuring relays and protection equipment – Part 26: Electromagnetic compatibility requirements. Geneva: IEC, 2023.

4. IEC 61000-4-30:2025. Electromagnetic compatibility (EMC) – Part 4-30: Testing and measurement techniques – Power quality measurement methods. Geneva: IEC, 2025.

5. IEC 61131-3:2025. Programmable controllers – Part 3: Programming languages. Geneva: IEC, 2025.

6. Siemens AG. SIMATIC S7-1200 Programmable Controller. System Manual. V4.6, 11/2022, A5E02486680-AK. 1620 p.

7. OMRON Corporation. Technical Explanation for Solid-state Relays: zero-cross function, leakage current, surge current and heat dissipation. 2024. 14 p.

8. Gencer Ö.Ö., Öztürk S., Karaarslan K. Performance of an Over/Under Voltage Relay at Non-sinusoidal Conditions // Proc. IEEE MELECON. 2006. P. 1102–1105.

9. Zubkov O., Svyd I., Vorgul O. Features of the Digital Filters Implementation on STM32 Microcontrollers // MC&FPGA. 2021. DOI: 10.35598/mcfpga.2021.001.

10. IEC 61131-2:2017. Industrial-process measurement and control – Programmable controllers – Part 2: Equipment requirements and tests. Geneva: IEC, 2017